New water vapor line parameters in the 26000-13000 cm-1 region — Source link

Pierre-François Coheur, Sophie Fally, Michel Carleer, Cathy Clerbaux ...+5 more authors

Institutions: Université libre de Bruxelles, Belgian Institute for Space Aeronomy

Topics: HITRAN, Water vapor, Radiative transfer, Line (formation) and Buffer gas

Related papers:

- The determination of an accurate isotope dependent potential energy surface for water from extensive ab initio calculations and experimental data

- The HITRAN 2008 molecular spectroscopic database

- Convergence testing of the analytic representation of an ab initio dipole moment function for water: Improved fitting yields improved intensities

- The Water Vapor Spectrum in the Region 8600-15 000 cm ¡1 : Experimental and Theoretical Studies for a New Spectral Line Database I. Laboratory Measurements

- Water vapour line assignments in the 9250–26 000 cm–1 frequency range

New water vapor line parameters in the $26000-13000\,\text{cm}^{-1}$ region

Pierre-François Coheur[a,1], Sophie Fally[a], Michel Carleer[a], Cathy Clerbaux[a,2], Réginald Colin[a,*], Alain Jenouvrier[b], Marie-France Mérienne[b], Christian Hermans[c], Ann Carine Vandaele[c]

[a]*Laboratoire de Chimie Physique Moléculaire, Université Libre de Bruxelles, 50 Av. F.D. Roosevelt, B-1050 Brussels, Belgium*
[b]*Groupe de Spectrométrie Moléculaire et Atmosphérique, UFR Sciences, Moulin de la Housse B.P. 1039, 51687 Reims Cedex 2, France*
[c]*Institut d'Aéronomie Spatiale de Belgique, Av. Circulaire 3, B-1180 Brussels, Belgium*

Abstract

The radiative properties of water vapor play an important role in the physical and chemical processes occurring in the atmosphere. Accurate knowledge of the line parameters for this species is therefore needed. This work presents new measurements of water vapor line parameters in the $26\,000-13\,000\,\text{cm}^{-1}$ spectral region. The measurements were obtained by combining a high-resolution Fourier transform spectrometer with a long-path absorption cell, thus allowing the observation of very weak, previously unobserved, lines. A total of more than 9000 lines have been identified and their position, integrated cross section and self-broadening parameter have been determined. The dependence of the line parameters on nitrogen buffer gas pressure (0–800 hPa) has also been studied. The complete line list presented here is primarily compared to the HITRAN spectroscopic database, most frequently used in atmospheric calculations. © 2002 Elsevier Science Ltd. All rights reserved.

---

* Corresponding author. Fax: +32-2-650-4232.
E-mail address: rcolin@ulb.ac.be (R. Colin).

1. Introduction

Water in all its three phases has a key role in the climate system of the Earth. Water vapor, more particularly, is the most abundant greenhouse gas, an important chemical reactant and a carrier of latent heat. Being also the most variable atmospheric species, it intervenes in the climate system through different feedback mechanisms that are still not completely understood, due to the lack of observations. These are made difficult as a result of the inhomogeneous horizontal and vertical distribution of the species in the atmosphere. At present, the measurements of atmospheric water vapor are best performed from space-borne instruments (balloon-borne radiosondes or satellite-borne infrared or microwave sensors), which give either good horizontal or vertical resolution. The satellite measurements require high-quality laboratory data, which are not always available. Accurate spectroscopic measurements are in particular needed to obtain information on the absorption properties of atmospheric water vapor, which are important, among other things, to understand the Earth's energy balance. This problem has gained interest in recent years, since water vapor was proposed as a possible candidate for the "missing absorber" [1], that is the species, which is responsible for the excess of absorption when observations are compared to models (see, for example, [2]). The rational for this suggestion stems from the fact that water vapor has a complex and dense vibrational absorption spectrum, extending from the infrared to the near ultraviolet and characterized by a large number of weak lines, which have not all been identified. This suggestion that water vapor is the "missing absorber" has, however, been contradicted by recent calculations [3], which were shown to agree satisfactorily with the observations.

In the infrared below 4500 cm^{-1}, the spectroscopy of water vapor has been studied thoroughly and line parameters, generally of good quality, are readily available through the HITRAN [4,5] or GEISA [6] databases. Recent efforts in this spectral region were especially aimed at a better understanding of the pressure dependence of the line profile [7–9]. In the near infrared, above 4500 cm^{-1}, it is believed that the line lists implemented in the databases are quite extensive but, for some parameters, not sufficiently accurate [10]. It is in the visible and near ultraviolet, where the absorption is weak as compared to the infrared, that the data are the most incomplete [10]. A precise quantitative analysis of the absorption of water vapor in the visible spectral range is, however, particularly important for the atmospheric radiative budget, as it produces an attenuation of the solar radiation at its maximum of emission. A good knowledge of the weak lines in this visible region is also required for the retrieval of other atmospheric gases absorbing in the same spectral range, as for instance NO_2 [11]. At present, the most complete sets of water vapor line parameters available for the visible region are those of Camy-Peyret et al. [12] and of Mandin et al. [13], between $25\,250$ and $16\,500$ and $16\,500$ and $13\,200 \text{ cm}^{-1}$, respectively. The pressure and temperature effects have, however, not been studied in these earlier works. The line parameters measured by these groups have been implemented in the HITRAN database, where additional calculated values for water have also been added. Recently, in response to an announcement of opportunity of the European Space Agency [14], a new water vapor line list covering the spectral range from $20\,000$ to 8000 cm^{-1} has been constructed [15] and partly published [16]. Still in a preliminary form, this database (referred to as the ESA database in the following) is very extensive but includes a mixture of HITRAN lines, experimental measurements and calculations. Hence, none of the HITRAN and ESA database appears to be homogeneous over the entire spectral range. Aside the databases, some recent measurements have improved the line parameters in restricted spectral regions. In particular, the red portion of

the water vapor absorption spectrum has been analyzed by the use of laser techniques [17–20], which provide both high-resolution and long absorption path-length. However, these techniques are generally limited to a narrow spectral interval and are not fully adequate for determining absolute line intensities, because of the difficulty encountered in measuring the total absorption path with good accuracy. In the $13\,200$ cm^{-1} spectral region, Grossmann and Browell [17,18] have provided an extensive set of intensities and broadening parameters for water vapor in different buffer gases. In the blue region, Harder and Brault [11] have measured line intensities for water vapor lines lying between $22\,721$ and $22\,230$ cm^{-1} (atmospheric window for the NO_2 retrieval), which they subsequently used to calibrate the water vapor lines of an atmospheric solar spectrum recorded at the Kitt Peak National Observatory. This procedure allowed the authors to measure parameters for about 40% more lines than in the work of Camy-Peyret et al. [12], suggesting, as expected, that the line lists implemented in the databases could still be improved by new laboratory measurements.

It is the aim of this work to give a homogeneous and extensive set of water vapor line parameters in the region $26\,000$–$13\,000$ cm^{-1}. To do this, we have performed absorption measurements of pure and nitrogen diluted water vapor by using high-resolution Fourier transform spectroscopy and a long multiple reflection absorption cell. This paper is a development of previous work undertaken by our group [21,22], in which the spectroscopic assignments of water vapor in the visible and near ultraviolet are given. In the present contribution, we focus on the measurement of the line integrated absorption cross section and width and on the dependence of the line parameters with the nitrogen buffer gas pressure. A special emphasis is put on the comparison of the line parameters measured is this work with those implemented in the HITRAN and ESA spectroscopic databases.

2. Experimental

A detailed description of the experimental setup and procedure has been given previously [21]. Briefly, the absorption spectra of water vapor were recorded using a high-resolution Fourier Transform Spectrometer (Bruker 120M) coupled to a White multiple-reflection absorption cell of 50 m base path. With a 450 W high-pressure Xenon arc lamp taken as the light source, a total absorption path of 602.32 m was selected in order to maximize the signal-to-noise ratio (S/N). All spectra were recorded at room temperature (291.3 K) and at a resolution of 0.06 cm^{-1} (15 cm maximum optical path difference). A silicon diode was used to cover the visible part of the spectrum ($23\,000$–$13\,000$ cm^{-1}), where the co-addition of 2048 interferograms (total recording time of 12 h) proved to be adequate, leading to a S/N ratio of 2500 (expressed as the maximum signal amplitude divided by twice the root-mean-square noise amplitude). A GaP detector was used above $23\,000$ cm^{-1}, where twice the number of interferograms was accumulated to produce a similar S/N ratio to that obtained in the lower wavenumber region. Different optical filters were used in combination with the silicon and GaP detectors.

The pure water vapor spectra were measured by introducing 18.5 hPa into the absorption cell, in order to allow the observation of weak lines while avoiding condensation on the mirrors and on the cell windows. The N_2 diluted water vapor mixtures were prepared by progressively adding nitrogen into the cell filled with water vapor. Four dilutions, characterized by 170, 337, 569 and 802 hPa total pressure were analyzed in this work. The temperature within the cell was measured with three platinum wire thermometers and the pressure with an MKS Baratron capacitance manometer.

3. Data analysis

A Fourier transform interpolation factor of 16 was first applied to all the recorded spectra to ensure that the lines are well represented. From all of these, the atmospheric water absorption, occurring in the 6 m long absorption path between the cell and the entrance of the spectrometer, was carefully removed, as described earlier [23]. This external contribution to the absorption was typically of the order of 1% of the total water vapor absorption, depending on the humidity within the room.

The wavenumber scale was calibrated using the iodine lines. All spectra were first calibrated with respect to one another, in air, using the molecular atmospheric oxygen lines around $13\,000$ cm^{-1}. The corresponding wavenumber scale was then adjusted by comparing a set of iodine line positions between $16\,000$ and $19\,000$ cm^{-1}, recorded simultaneously with one of the water spectrum, with those listed in [24,25], but transformed to air using Edlén's formula [26]. The wavenumber scale was transformed into vacuum wavenumbers by applying to the line positions a fifth degree polynomial based on Edlén's formula.

The water vapor line parameters were extracted from the spectra using the WSPECTRA program [27], which fits one by one the lines to a theoretical profile, convolved by the instrumental function. The baseline is also fitted by WSPECTRA. The program operates in two steps, each relying on a non-linear least-squares procedure. In the first step, both a Gaussian and a Lorentzian contribution to the profile are fitted, with the amount of Lorentzian width being characterized by a so-called damping factor. Based on these first values of the line parameters, the program refits the line to a chosen profile (Rautian–Sobel'man [28] or Galatry [29]), with the Gaussian width fixed to its calculated value, depending on temperature and wavenumber. The results of the fit are expressed in terms of the line position v, area A and Lorentzian full-width at half-maximum Γ, all in wavenumber units. In the case of the Rautian–Sobel'man and Galatry line profiles, an additional narrowing parameter is fitted. The line area and Lorentzian width are then converted into more conventional line integrated cross sections S_σ (cm molecule^{-1}) and pressure-broadening parameters γ (cm^{-1} atm^{-1}).

The line integrated cross sections (S_σ) and self-broadening parameters (γ_{self}) were determined from the pure water vapor spectra, except when the lines were saturated. In this case, the lowest dilution providing non-saturated lines was used for the measurement of the cross section. In regions where several pure water vapor spectra were recorded using different combinations of detectors and filters, S_σ and γ_{self} were obtained by calculating the averaged value of the individual parameters. In the averaging procedure, the root mean square (RMS) value of the fit was used as the weighting factor. The relationships used to transform line areas and Lorentzian line widths into line integrated absorption cross sections and self-broadening parameters are as follows:

$$S_\sigma = A \frac{P_0 T}{n_{\text{L}} T_0 P l}, \tag{1}$$

$$\gamma_{\text{self}} = \frac{\Gamma}{2P}, \tag{2}$$

where T and P are the temperature and the pressure in the cell (T being 291.3 K), $T_0 = 273.15$ K, P_0 is one atmosphere, l is the absorption path length in cm and n_{L} is the Loschmidt number ($n_{\text{L}} = 2.68676 \times 10^{19}$ molecule cm^{-3}).

The N_2-broadening parameters (γ_{N_2}) and frequency shifts (δ_{N_2}, in cm^{-1} atm^{-1}) are considered to be related to the partial H_2O and N_2 pressures in the cell by the usual linear expressions

$$\Gamma/2 = (\gamma_{self} \times P_{H_2O}) + (\gamma_{N_2} \times P_{N_2}),$$ (3)

$$v_{P_{N_2}} = v + (\delta_{N_2} \times P_{N_2}),$$ (4)

where v is the wavenumber measured from the pure water vapor spectrum at 18.5 hPa. γ_{N_2} and δ_{N_2} were accordingly calculated by solving the systems of equations, each defined by the total pressure, using general linear least-squares fits [30]. In these calculations, the statistical weights were taken as the RMS values of the fitted line parameters. The RMS values resulting from the least-squares procedure was adopted as the final statistical uncertainties on the line parameters.

For the comparison with literature and the databases, we have converted the line parameters measured here at 291.3 K (T_1) to the temperature T_2, usually 296 K, by using the following approximate relations:

$$S_\sigma(T_2) = S_\sigma(T_1) \left(\frac{T_1}{T_2}\right)^{3/2} e^{-\frac{hc}{k}\frac{E''(T_1-T_2)}{T_1 T_2}},$$ (5)

$$\gamma(T_2) = \left(\frac{T_1}{T_2}\right)^n \gamma(T_1),$$ (6)

$$\delta(T_2) = \left(\frac{T_1}{T_2}\right)^n \delta(T_1).$$ (7)

A value of 0.6 is used for n. As discussed in [9], although this value of n may not be correct for all transitions, it has only a weak influence on the line parameters: an error of 50% on n would only produce a difference of 0.5% on the retrieved parameters.

The uncertainties in wavenumbers, cross sections, half-widths and pressure shifts have been estimated. First, a statistical uncertainty resulting from the fitting procedure was obtained for each parameter, as detailed above (this uncertainty on the parameters is different from line to line and generally substantially larger for the weak or blended lines than for the strong and well-resolved lines). Then, in addition to the statistical error, a systematic error arising from the uncertainties on the pressure, the temperature, the path length and the calibration procedure was taken into account. Assuming uncertainties for the temperature and pressure measurements of 1% and on the path length of 0.5%, we estimate the systematic uncertainty on the position and the cross sections to be 2×10^{-5}% and 2.5%, respectively. For the pressure-dependent parameters (γ_{self}, γ_{N_2} and δ_{N_2}), the systematic uncertainty is 1%. The absolute uncertainty on the parameters can be recalculated considering both types of uncertainties.

4. Results and discussion

An overview of the water vapor absorption spectrum from 26 000 to 13 000 cm^{-1} is presented in Fig. 1, with the bands identified by their associated polyad number (v and δ refer to the stretching and bending modes, respectively). The two overlapping regions, corresponding to the two main
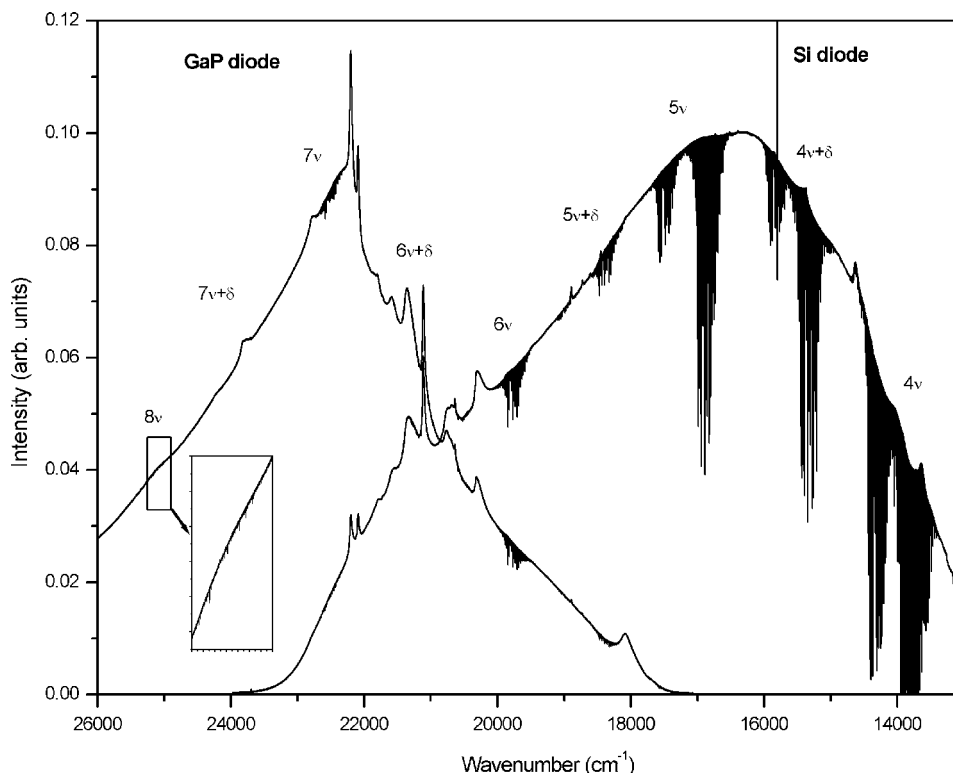
Fig. 1. Raw pure water vapor spectrum (18.5 hPa) in the visible and near ultraviolet region. ν and δ are the stretching and bending modes, respectively.

combinations of detectors and filters used are shown. From Fig. 1, it is seen that the band intensities, strong in the visible, decrease at higher wavenumbers. The complete list of the lines identified is made available in electronic format from the "Laboratoire de Chimie Physique Moléculaire" website (http://www.ulb.ac.be/cpm/). The list presents each line parameter with its associated statistical uncertainty (3σ), the rotational and vibrational assignments and the energy of the lower state. The additional last two columns in the electronic file give the reference used for the line assignment and an indication if the line is saturated at 18.5 hPa and if it belongs to the $H_2^{18}O$ isotope. A formatted HITRAN-like table can also be obtained from the website.

4.1. Line identification, position and assignment

Within the nine polyads observed, 9353 lines have been identified and fitted (see Table 1 for a summary of the observations). This is slightly less than what was given in our previous publications [21,22], essentially because the analysis of several spectra, recorded under different pressure conditions, allows a better discrimination of the weak features from the noise. Among all the lines identified, only about half are present in the HITRAN database, the main improvement in the line parameters being obtained in the blue region (26 000–20 000 cm^{-1}). It should be noted that 76 lines are listed in HITRAN but are not observed in the present work and also that some features have

Table 1
Summary of the results and comparison with the most recent literature data. $S_{\sigma\,min}$ and $S_{\sigma\,max}$ refer to the minimum and maximum absorption cross sections

	This work (291.3 K)	HITRAN 2000 (296 K)	ESA (296 K)	
			From experiment	From theory
Spectral range (cm^{-1})	26 000–13 000	22 656–13 000	20 000–13 000	
Number of lines	9353	4610	2199	9588
Number of assigned lines	6084	3155	1828	9588
$S_{\sigma\,min}$ (cm molecule^{-1})	4.47×10^{-28}	2.60×10^{-27}	3.00×10^{-28a}	1.00×10^{-28}
$S_{\sigma\,max}$ (cm molecule^{-1})	3.80×10^{-23}	3.44×10^{-23}	5.20×10^{-23}	5.49×10^{-24}

[a]Three lines having a smaller value than $S_\sigma = 3.00 \times 10^{-28}$ are listed in the experimental values of ESA.

been fitted to a single line in this work but are assigned to a doublet in HITRAN. The ESA line list is much more extensive than ours but is a mixture of measured (2199 lines), calculated (9588 lines) as well as HITRAN-based values (2301 lines), over a narrower 20 000–13 000 cm^{-1} spectral region.

The vacuum wavenumbers agree with those of our earlier works [21,22] to better than 5×10^{-4} cm^{-1} on average, which is smaller than the error limit considered here. A similar agreement exists with respect to other publications [11–13,17,18,31], including the HITRAN database and the experimental measurements of the ESA database. Based on the good agreement in the line positions, for most of the lines we have used the assignments of the previous theoretical analysis [21,22]. In a few cases, the line assignments of [15] were taken because no match with [21,22] was found. This results in the fact that in some cases, a same assignment is given to two different lines. With the exception of a few lines originating from the first excited vibrational level (0 1 0), all lines originate from the vibrational ground state and end on 67 different excited vibrational levels, belonging to the polyads lying between 4v and 8v.

4.2. Cross sections

The determination of the line cross sections is an important result of this work and we have therefore taken special care in measuring very weak lines. The intensity limits with the experimental conditions chosen here are characterized by line integrated cross sections ranging between 4.47×10^{-28} and 3.80×10^{-23} cm molecule^{-1} (Table 1). The lower limit presents a significant improvement in regard to the earlier measurements compiled in HITRAN.

The cross sections can be compared line-by-line or integrated over larger spectral ranges, e.g., each polyad or the entire region investigated. The comparison of integrated cross sections taken from our measurements with those of the latest version of HITRAN and the recent ESA database is given in Table 2 and plotted in Fig. 2. These results show that the integrated cross section over the entire spectral range investigated (2.03×10^{-21} cm molecule^{-1}) is about 5% larger than that obtained with the HITRAN values. However, it is to be noted from Table 2 that the intensity is in great part carried by the 4v polyad and to a lesser extent by the 4$v + \delta$ and 5v polyads. The remaining polyads

Table 2
Number of lines (N) and integrated cross sections (S_σ in cm molecule^{-1}) measured for each polyad in this work and in the HITRAN and ESA databases. The theoretical values in ESA are given for unobserved lines

| Polyad | This work (291.3 K) | | HITRAN (296 K) | | ESA (296 K) | | | |
| | | | | | Experiment[a] | | Theory | |
	N	S_σ	N	S_σ	N	S_σ	N	S_σ
$4v$	3189	1.68×10^{-21}	2101	1.58×10^{-21}	910	1.70×10^{-21}	7304	5.86×10^{-23}
$4v + \delta$	1641	1.26×10^{-22}	695	1.27×10^{-22}	1110	1.31×10^{-22}	1842	5.48×10^{-24}
$5v$	2119	1.80×10^{-22}	1027	1.83×10^{-22}	1585	1.91×10^{-22}	364	3.10×10^{-24}
$5v + \delta$	776	1.43×10^{-23}	356	1.38×10^{-23}	546	1.55×10^{-23}	68	2.45×10^{-26}
$6v$	888	2.60×10^{-23}	279	2.28×10^{-23}	349[b]	2.27×10^{-23}		
$6v + \delta$	257	1.92×10^{-24}	80	1.40×10^{-24}				
$7v$	373	4.97×10^{-24}	72	3.50×10^{-24}				
$7v + \delta$	45	2.28×10^{-25}						
$8v$	65	8.63×10^{-25}						
Total	9353	2.03×10^{-21}	4610	1.93×10^{-21}	4500	2.06×10^{-21}	9588	6.72×10^{-23}

[a]Includes HITRAN values (2301 lines in total) and new measurements.
[b]Restricted to wavenumbers below $20\,000$ cm^{-1}.

contribute by less than 3% to the total absorption in the visible. It is, therefore, not surprising that the larger integrated cross sections obtained in our work with respect to HITRAN is in part due to systematic deviations for the stronger water vapor lines, which are on the average 3% more intense in our measurements (Fig. 3). On the contrary our weak lines ($S_\sigma < 6.5 \times 10^{-25}$ cm molecule^{-1}) have smaller integrated cross sections (Fig. 3) but, because of their large number, they produce a further increase of total absorption when compared to HITRAN. In summary, for all the lines in common with HITRAN above $13\,000$ cm^{-1}, we have measured an integrated cross section of 1.98×10^{-21} cm molecule^{-1}, which is to be compared to 1.93×10^{-21} obtained from HITRAN. The measurement of about 4700 new weak lines increases thus the total integrated cross section by 2%. The comparison with the ESA line list can be made in a similar manner. First, taking the experimental values of ESA (including their HITRAN lines), we observe that despite a smaller number of lines and a restricted spectral interval, the ESA integrated cross section is 2% larger than ours (Table 2 and Fig. 2). Here again the reason is to be found in the stronger lines of the $4v$ polyad, which have individually a larger cross section (about 6% on average) according to the ESA new measurements. The myriad of very weak lines obtained from the ESA calculations contributes to the total integrated cross section by an additional 3%. It is to be noted, however, that the calculations show some important discrepancies with our experimental measurements. This is especially obvious for lines belonging to the $4v$ polyad, for which the intensity limit of the measured cross sections in the ESA database has been placed at 10^{-25} cm molecule^{-1} in some spectral intervals: all measured lines of ESA show indeed a satisfactorily agreement with our data, in contrast to the calculated values (Fig. 4). For atmospheric calculations relating to the Earth's energy budget, it seems thus that these calculated lines should be used with caution.

It should also be remarked that our line integrated cross sections agree well with those of other recent measurements, which were performed over limited spectral intervals, such as those of Harder
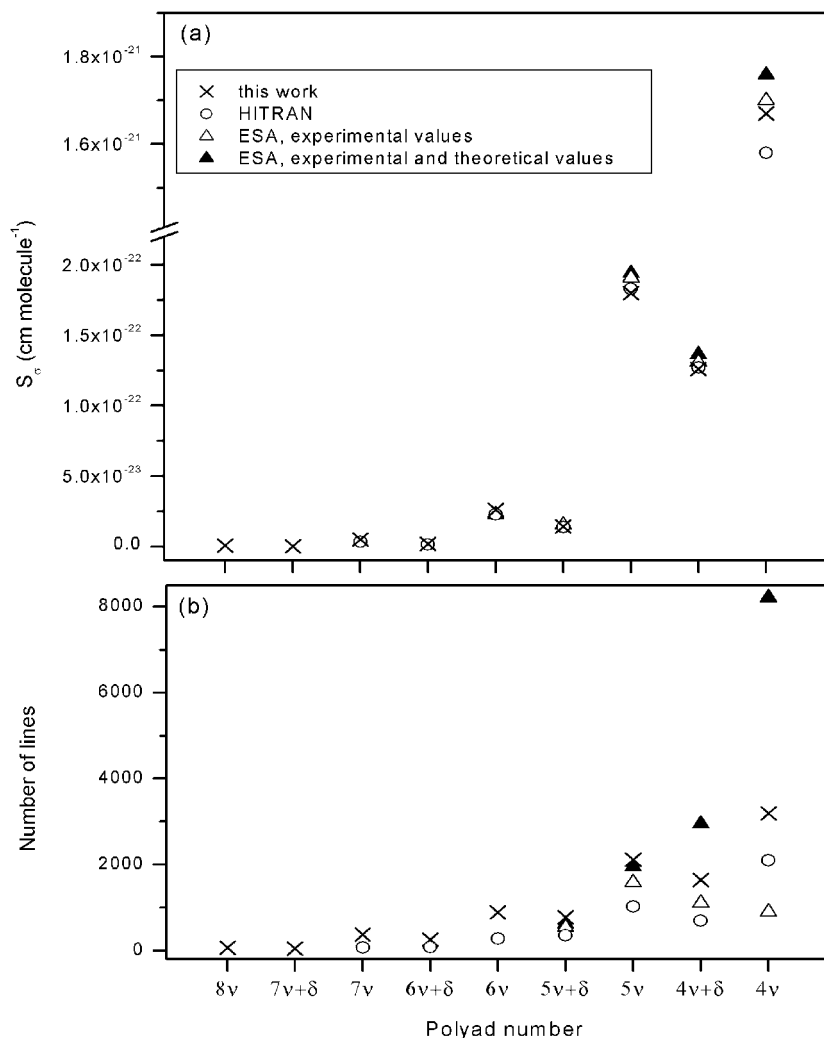
Fig. 2. Integrated cross sections in cm molecule^{-1} (a) and number of lines (b) for each polyad. In the ESA experimental values, about half of the lines originate from HITRAN.

and Brault in the 22 500 cm^{-1} region [11], Grossman and Browell [18], Brown and Plymate [31] and Singh and O'Brien [20] around 13 200 cm^{-1}. This good agreement with independent measurements of weak and strong lines lying in different spectral ranges shows the reliability of our measurements, which, compared to these works, presents the advantage of covering an unusually large range of intensities (4.5×10^{-28}–3.8×10^{-23} cm molecule^{-1}) over the entire visible spectral region.

4.3. Self-broadening parameters

We have found that for the region investigated here, the use of a Voigt line shape produces generally an equally good agreement as the use of a Rautian–Sobel'man or a Galatry line profile,
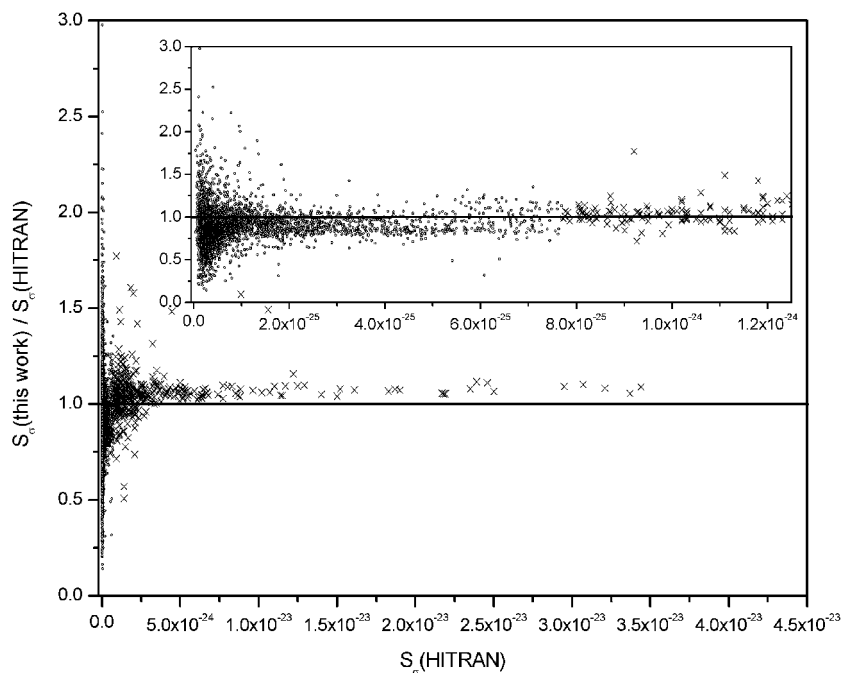
Fig. 3. Comparison of the line integrated cross sections with respect to the HITRAN values (S_σ, given in cm molecule^{-1} at 296 K). The inset gives an expanded portion of the plot for cross sections smaller than 1.25×10^{-24} cm molecule^{-1}. Two distinct regions are obvious: Values of 1.03 and 0.90 are measured for the ratio S_σ(this work)/S_σ(HITRAN) above (crosses) and below (circles) the value $S_\sigma = 7 \times 10^{-25}$ cm molecule^{-1}, respectively.

even though line-narrowing effects in water vapor have been observed and analyzed thoroughly in the infrared [7–9]. The Voigt line profile was thus applied systematically, as in previous measurements [9], and also because the accurate determination of the narrowing parameter would have been hardly accessible for most of the weak lines. In fact, for the weak lines, the measurement of the self-broadening parameter γ_{self} is difficult and the statistical uncertainty associated with this parameter in the list presented here may be relatively large. In the case where the fitting procedure found no Lorentzian contribution to the line profile, no value of γ_{self} is given in the present list. It should finally be noted that some of the γ_{self} values listed are much larger than the average value, indicating that the observed feature may be a multiplet of lines, unresolved with the experimental conditions chosen.

In the spectral region examined, a mean value of $\gamma_{self} = 0.44$ cm^{-1} atm^{-1} is obtained by taking all experimental measurements weighted with their associated statistical errors. However, it is known that the self-broadening parameter varies with the rotational and vibrational quantum numbers [9,32], so that this mean value has no real physical meaning. For instance, we have found that an average value of γ_{self} measured within each polyad increases as the polyad number increases from $4v$ to $8v$ (Fig. 5). This could be due in part to the fact that the lines observed at higher energy involve more rotational levels of low J'', which are generally characterized by larger values of the broadening parameter [18]. However, a preliminary survey of the evolution of γ_{self} with J'' did not yield a clear-cut evolution, suggesting that other quantum numbers may have to be taken into account.

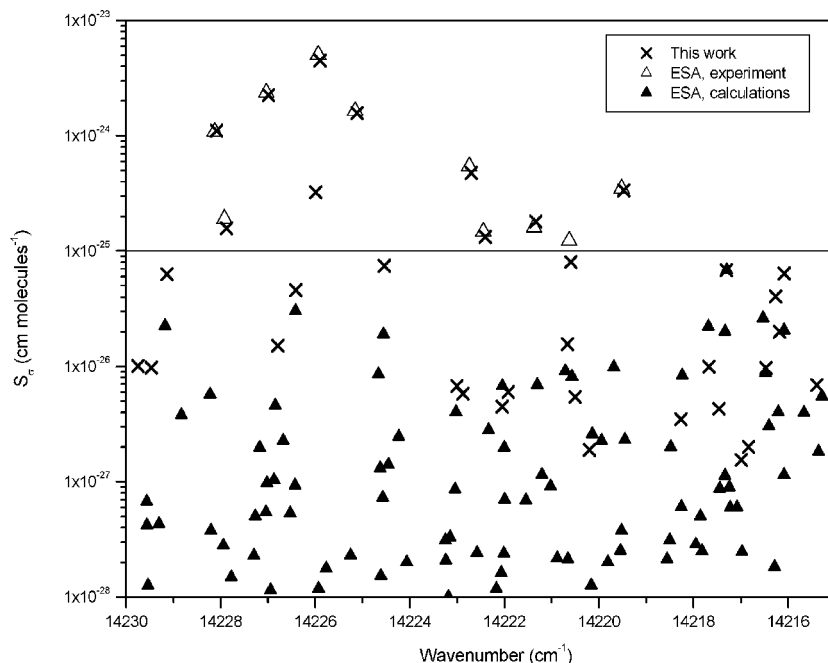Fig. 4. Comparison with the ESA experimental and calculated values of line cross section measurements in this work (14 230–14 215 cm^{-1} interval). The line at 10^{-25} cm molecule^{-1} represents the lower limit of the ESA experimental values in this spectral range.

Taken globally, our measured values of γ_{self}, transformed at 296 K using Eq. (6), agree very well ($< 1\%$) with those given in HITRAN. The comparison with the mean values calculated within each polyad is also satisfactory (Fig. 5) but the trend revealed with our data appears less marked with the HITRAN values. Large disagreements exist between our measurements and the new measurements of the ESA database. As far as the $4v$ polyad is concerned, the ESA values appear to be larger than ours and those of HITRAN by about 10% whereas for the higher polyads, their listed values are smaller than ours. The source of discrepancies with the ESA database is not clear at present. The water vapor line widths in a narrow portion of the visible region (13 970–13 550 cm^{-1}) have been studied thoroughly by Grossman and Browell [18]: their values of the self-broadening parameter for 170 lines having a cross section larger than 10^{-25} cm molecule^{-1} agree very well (to better than 2% on average) with our values, as shown in Fig. 6.

4.4. Pressure dependence

The dependence of the line width and of the line position with the N_2 buffer gas pressure has been examined in the pressure range of 18.5 (pure water vapor) to 802 hPa. As for γ_{self}, the measurements of the N_2-broadening parameter (γ_{N_2}) and of the wavenumber shift (δ_{N_2}) are subject to large uncertainties. Furthermore, most of the weak lines disappear in the noise when the N_2 pressure is increased, thus making it difficult and sometimes impossible to determine pressure-dependent parameters for these features.
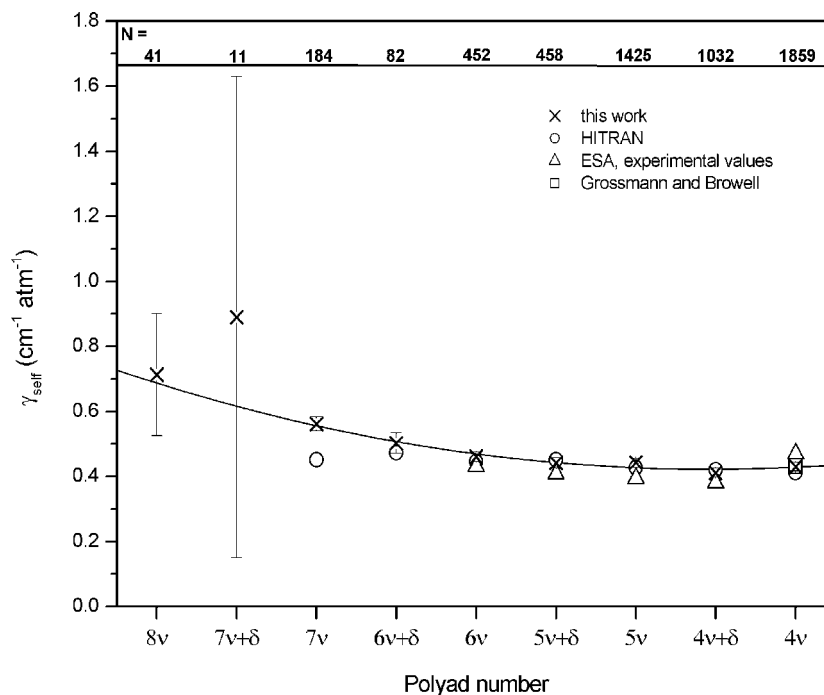
Fig. 5. Mean values of the self-broadening parameter γ_{self} (cm^{-1} atm^{-1}) calculated for each polyad. Only the ESA experimental values are considered. The fixed γ_{self} value reported in HITRAN for a large number of lines has not been taken into account. The value of N given for each polyad is the number of lines taken into account in the average.

The measurement of the absorption cross sections of the N_2-broadened lines agrees within 5% with the values obtained from the pure vapor spectra. However, because of the blending of lines at higher pressures, the measurement of intensities from the N_2-diluted spectra is subject to large uncertainties, justifying the exclusion of these measurements from the present line list.

The evolution of the line profile with the N_2 buffer gas pressure is illustrated in Fig. 7 for two well-defined lines at $19\,854$ cm^{-1}. It is evident that increasing the pressure produces a significant broadening of the lines, which can be quantified by the broadening parameter γ_{N_2} from Eq. (3). The values listed for γ_{N_2} are generally smaller than 0.2 cm^{-1} atm^{-1} but larger values have also been measured for weak lines or for lines overlapping each other. A mean value of 0.0896 cm^{-1} atm^{-1} is calculated for γ_{N_2} at 291.3 K over the entire visible spectral range. No obvious evolution with the polyad number nor with J'' has been observed. The values measured in this work are about 10% larger than those listed in HITRAN whereas the comparison with respect to the ESA database suffers similar problems as those discussed for the self-broadening parameter. Indeed, the ESA values are larger in the $4v$ polyad but systematically smaller in the higher polyads. Here again, it should be stressed that some of the values given in ESA may be computed and not measured. The comparison of our values for the N_2-broadening parameters with those of Grossman and Browell [17] is good, as was also the case for the self-broadening parameter (Fig. 6).

As far as we are aware, the dependence of the water vapor line positions with pressure in the visible spectral region above $14\,000$ cm^{-1} has never been reported before. In particular, the values of
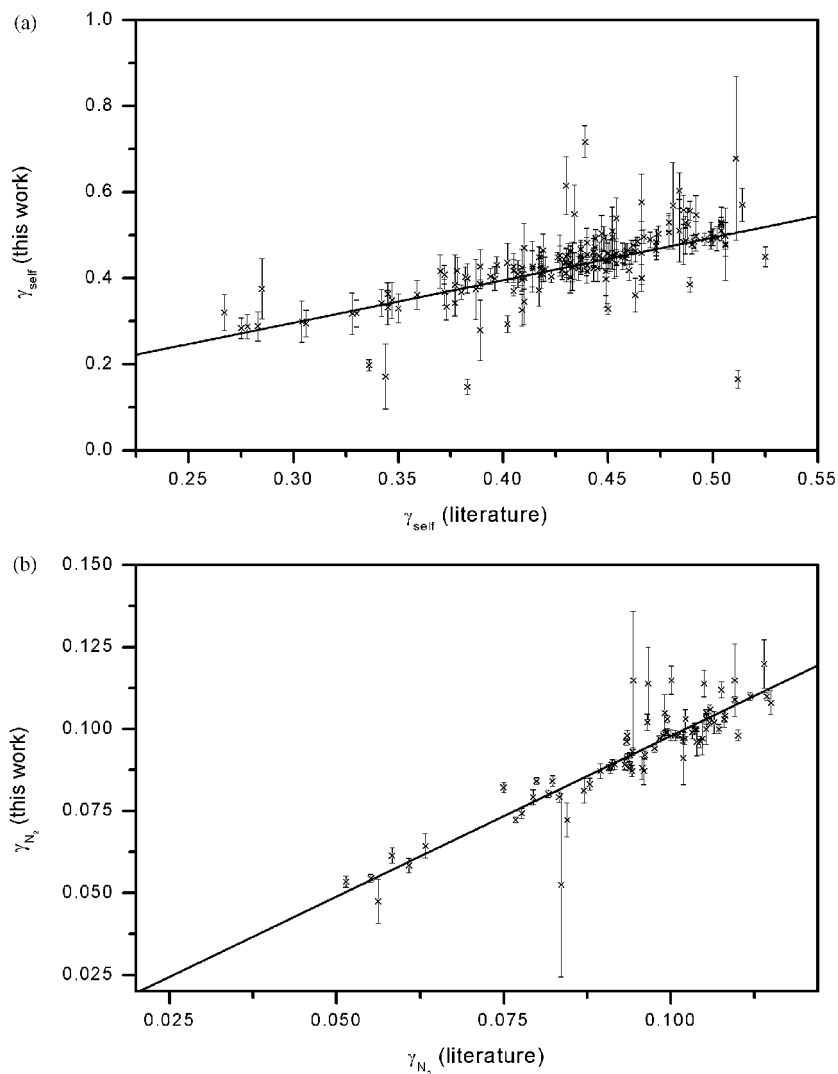
Fig. 6. Comparison of the measured self-broadening (a) and N_2-broadening (b) parameters (in $cm^{-1} atm^{-1}$ at 296 K) with the data reported in [17,18] between 13 966 and 13 558 cm^{-1}. The error bars are the statistical uncertainties (3σ) given in the present line list. The linear fit yield slopes of 0.99 and 0.98 for γ_{self} and γ_{N_2}, respectively.

δ_{N_2} are not listed in HITRAN or in the ESA database. Below 14 000 cm^{-1}, Grossman and Browell [17] have measured the wavenumber shifts for water vapor in different environments. The δ_{N_2} data reported by these authors for a small number of lines are very close to our values, obtained from Eq. (4) for about 7000 lines. As in [17], we observe indeed that the large majority of lines are shifted towards smaller wavenumbers with increasing N_2 buffer gas pressure. This is the case for example for the two lines plotted in Fig. 7. Furthermore, we have observed that the mean value of δ_{N_2} calculated for each polyad, follows an almost linear evolution with the polyad number, the
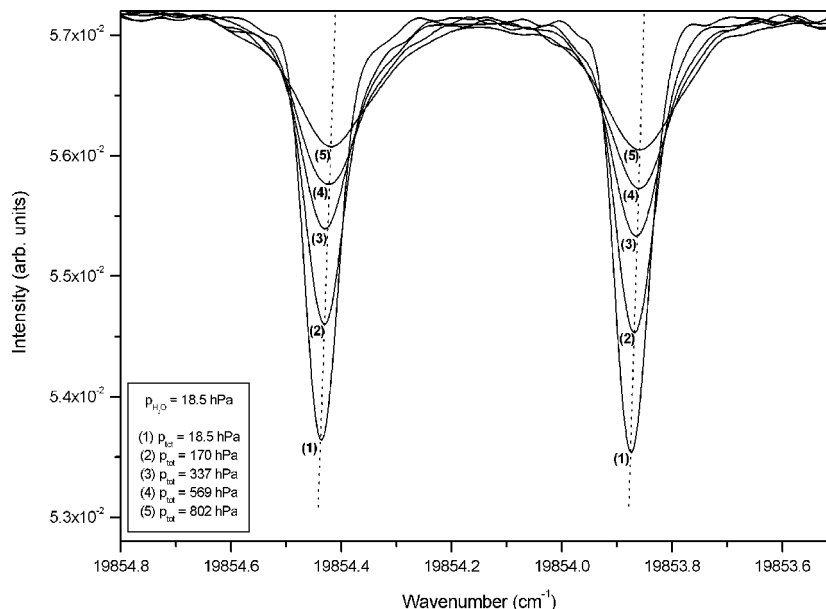
Fig. 7. Pressure dependence of the line profile for two well-defined lines of medium intensity (2×10^{-25} cm molecule^{-1}) belonging to the $6v$ polyad.

red shift being larger for the higher polyads (Fig. 8). There is no theoretical basis to explain this evolution, which requires obviously more detailed studies.

4.5. Atmospheric interest

The line parameters given in the present list have been checked for self-consistency, in the sense that they reproduce with a good accuracy both the pure and N_2-diluted spectra studied above. It should be stressed that in these simulations (made with the WINPROF program [33]), mean values of the pressure-broadening parameters ($\gamma_{self} = 0.44$ cm^{-1} atm^{-1} and $\gamma_{N_2} = 0.0896$ cm^{-1} atm^{-1}) have been adopted whenever the experimental values in the list were missing, regardless of the eventual dependence of these parameters with rotational and vibrational quantum numbers. It should also be noted that we have measured N_2-broadening parameters, which differ slightly from the air-broadening parameters that should be used in the atmospheric calculations: it is generally considered that γ_{N_2} has to be divided by a factor of 1.12 in order to reproduce the value of γ_{air} [17,34].

The line parameters measured in this work between 16 660 and 17 245 cm^{-1} have been used in a preliminary analysis of the GOME measurements (R. Lang et al., poster presented at the EGS symposium, Nice, France, 2000). In this spectral range, we have measured significantly more lines than what is listed in HITRAN, as is obvious from Fig. 9. It has been shown that the use of our line list in atmospheric forward calculations produces a good agreement with the GOME spectrum in this spectral region, and a significant improvement with respect to HITRAN. Systematic problems with the ESA line list were highlighted in this comparison with the GOME spectrum.
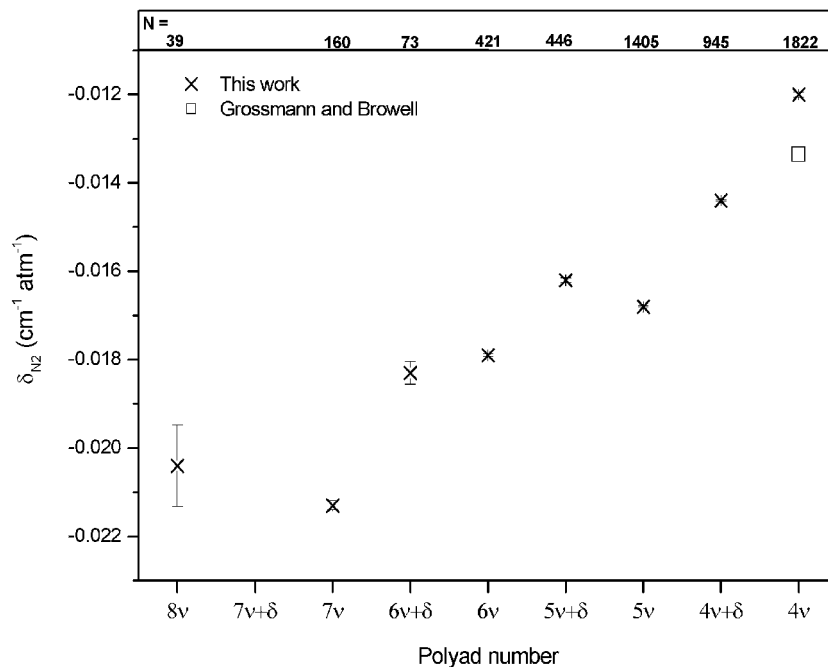
Fig. 8. Mean wavenumber shift parameter δ_{N_2} (cm^{-1} atm^{-1}), calculated for each polyad. The mean value obtained from 88 lines given in [17] and belonging to the $4v$ polyad is also shown. The value of N given for each polyad is the number of lines taken into account in the average.

5. Conclusion

We have given a new set of water vapor line parameters for the spectral region between 26 000 and 13 000 cm^{-1}. The measurements were obtained by combining high-resolution Fourier transform spectroscopy and a long absorption path of 600 m. With a total of 9353 lines identified and fitted, we have considerably improved the line list given in the HITRAN database, generally used in atmospheric calculations. Most of the lines have been assigned to rovibrational transitions, belonging to the polyads lying between $4v$ and $8v$. The calibrated line positions were shown to agree with previous studies and with HITRAN to better than 5×10^{-4} cm^{-1}, while the line cross sections showed discrepancies of the order of 5% when compared to HITRAN. The integrated cross sections over the spectral range investigated is 5% larger than that obtained with HITRAN values, with about half of this difference being directly attributed to the absorption of the newly identified water lines. The self-broadening parameters have been measured for a large number of lines and were shown to be in good agreement with literature. An evolution of the self-broadening parameter with the polyad number has been observed, but no definitive arguments to rationalize the observation have been proposed. The dependence of the line profile with nitrogen buffer gas pressure has been examined for pressures up to 800 hPa. A good agreement with HITRAN is observed for the broadening parameters while the wavenumber shifts have been measured for the first time over the visible portion of the spectrum: our results suggest that most of the lines are red-shifted with increasing
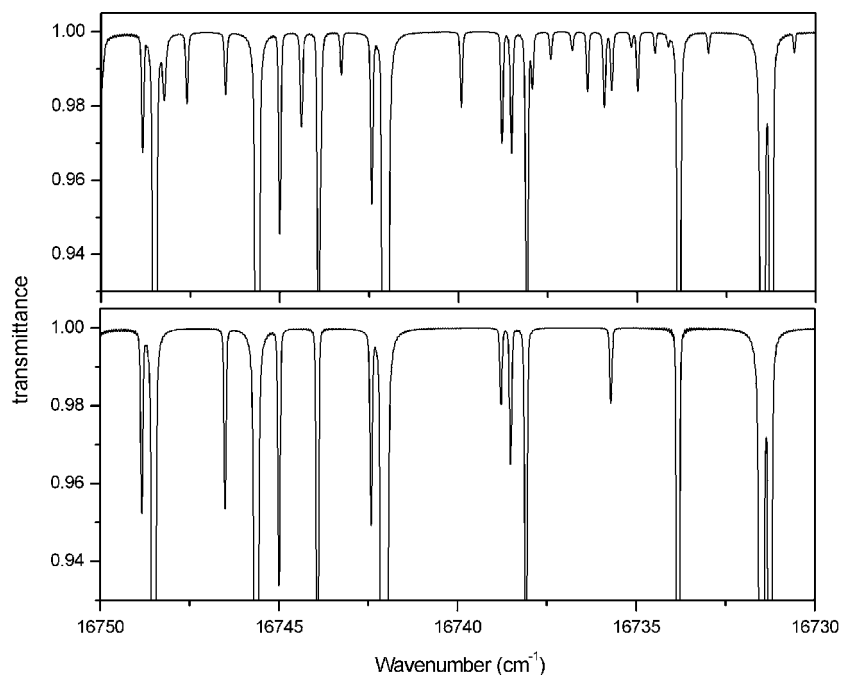
Fig. 9. Simulation of a pure water vapor spectrum with the line parameters obtained in this work (top) and those listed in HITRAN (bottom).

N_2 pressure and that this shift increases almost linearly with the polyad number. A comparison of our line parameters was also carried out with respect to the preliminary line list published for the European Space Agency (ESA), which includes both experimental and computed values. Although a satisfactory agreement with our data was found for the cross-sections, we have observed large discrepancies for the pressure-broadening parameters. It is to note that the ESA line list includes a very extensive set of calculated values for weak lines, which do not show a good agreement with our measurements, but which adds another 3% to the total absorption. These results highlight the importance of the weak lines in the total attenuation of solar light and illustrate the need to have an extensive set of line parameters for performing atmospheric calculations, especially in regard to radiative budgets. We believe that the line list presented in this work, which has the advantage of being, on the one hand, much more extensive than actual databases, with a cross section dynamic range of 10^5, and on the other hand, fully homogeneous for the entire visible region investigated, will improve the accuracy of upcoming atmospheric studies.

Acknowledgements

References

[1] Arking A. Science 1996;273:779–81.

[2] Ramanathan V, Vogelmann AM. Ambio 1997;26(1):38–46.

[3] Mlawer EJ, Brown PP, Clough SA, Harrison LC, Michalsky JJ, Kiedron PW, Shippert T. Geophys Res Lett 2000;27(17):2653–6.

[4] Rothman LS, Rinsland CP, Goldman A, Massie ST, Edwards DP, Flaud J-M, Perrin A, Camy-Peyret C, Dana V, Mandin J-Y, Schroeder J, McCann A, Gamache RR, Wattson RB, Yoshino K, Chance KV, Jucks KW, Brown LR, Nemtchinov V, Varanasi P. JQSRT 1996;60:665.

[5] Rothman LS, Barbe A, Benner C, Brown LR, Camy-Peyret C, Carleer M, Chance K, Clerbaux C, Dana V, Devi M, Fayt A, Flaud J-M, Gamache RR, Goldman A, Jaquemart D, Jucks KW, Lafferty W, Mandin J-Y, Massie ST, Newnham D. JQSRT, http://www.hitran.com/.

[6] Jaquinet-Husson N, Arié E, Ballard J, Barbe A, Bjoraker G, Bonnet B, Brown LR, Camy-Peyret C, Champion J-P, Chédin A, Chursin A, Clerbaux C, Duxbury G, Flaud J-M, Fourrié N, Fayt A, Graner C, Gamache R, Goldman A, Golovko V. JQSRT 1999;61:4205–54.

[7] Claveau C, Henry A, Hurtmans D, Valentin A. JQSRT 2001;68:273–98.

[8] Toth RA. J Mol Spec 2000;201:218–43.

[9] Toth RA, Brown LR, Plymate C. JQSRT 1998;59(6):529–62.

[10] ESA contract No 13048/98/NL/GD. Definition of observational requirements for support to a future earth explorer atmospheric chemistry mission. Appendix F. Spectroscopy 2001.

[11] Harder JW, Brault JW. J Geophys Res 1997;102(D5):6245–52.

[12] Camy-Peyret C, Flaud J-M, Mandin J-Y, Chevillard J-P, Brault J, Ramsay DA, Vervloet M, Chauville J. J Mol Spec 1985;113:208–28.

[13] Mandin J-Y, Chevillard J-P, Camy-Peyret C, Flaud J-M. J Mol Spec 1986;116:167–90.

[14] ESA contract 13 312/99/NL/SF. Measurement of H_2O absorption cross-sections for the exploitation of GOME data.

[15] http://www.msf.rl.ac.uk/esa-wv.

[16] Belmiloud D, Schermaul R, Smith KM, Zobov NF, Brault JW, Learner RCM, Newnham DA, Tennyson J. Geophys Res Lett 2000;27(22):3703–6.

[17] Grossmann BE, Browell EV. J Mol Spec 1989;138:562–95.

[18] Grossmann BE, Browell EV. J Mol Spec 1989;136:264–94.

[19] Kalmar B, O'Brien JJ. J Mol Spec 1998;192:386–93.

[20] Singh K, O'Brien JJ. J Mol Spec 1994;167:99–108.

[21] Carleer M, Jenouvrier A, Vandaele AC, Bernath PF, Mérienne M-F, Colin R, Zobov NF, Polyansky OL, Tennyson J, Savin SA. J Chem Phys 1999;111(6):2444–50.

[22] Zobov NF, Belmiloud D, Polyansky OL, Tennyson J, Shirin SV, Carleer M, Jenouvrier A, Vandaele AC, Bernath PF, Mérienne M-F, Colin R. J Chem Phys 2000;113(4):1546–52.

[23] Coheur P-F, Fally S, Vandaele AC, Hermans C, Jenouvrier A, Carleer M, Merienne M-F, Clerbaux C, Colin R. Absolute intensities of water vapor lines in the near-ultraviolet and visible regions. In: Russel JE. Klaus Schäfer, Lado-Bordowski O, editors. Remote sensing of clouds and the atmosphere, vol. V. EOS/SPIE Proceedings series, 2001. p. 97–105.

[24] Gesternkorn S, Luc P. Atlas du spectre d'absorption de la molécule d'iode. France: Editions du CNRS, 1978.

[25] Gesternkorn S, Luc P. Rev Phys Appl 1978;8:791.

[26] Edlén B. Metrologia 1966;2:71.

[27] Carleer M. Wspectra: a Windows program to measure accurately the line intensities of high resolution Fourier Transform spectra. In: Russel JE, Klaus Schäfer, Lado-Bordowski O, editors. Remote sensing of clouds and the atmosphere, vol. V. EOS/SPIE Proceedings series, 2001. p. 337–42.

[28] Rautian SG, Sobel'man II. Soviet Phys Uspekhi 1967;9(5):701–16.

[29] Galatry L. Phys Rev 1961;122(4):1218–23.
[30] Press WH, Teukolsky SA, Vetterling WT, Flannery BP. Numerical recipes in Fortran 77: the art of scientific computing. Melbourne, Australia: Cambridge University Press, 1996.
[31] Brown LR, Plymate C. J Mol Spec 2000;199:166–79.
[32] Brown LR, Plymate C. JQSRT 1996;56(2):263–82.
[33] Hurtmans D. Etude d'intensités spectrales dans des molécules d'intérêt atmosphérique. thesis, Université Libre de Bruxelles, 1995.
[34] Malathy Devi V, Benner CD, Rinsland CP, Smith MAH, Sidney BD. J Mol Spec 1986;117:403–7.